



Tyrosinase inhibitory mechanism and anti-browning properties of novel kojic acid derivatives bearing aromatic aldehyde moiety

Zhiyun Peng^{a,b}, Guangcheng Wang^d, Yan He^a, Jing Jing Wang^{b,c,*}, Yong Zhao^{b,**}

^a Clinical Trails Center, The Affiliated Hospital of Guizhou Medical University, Guiyang, China

^b College of Food Science and Technology, Shanghai Ocean University, Shanghai, 201306, China

^c Guangdong Provincial Key Laboratory of Intelligent Food Manufacturing, Foshan University, Foshan, 528225, China

^d Guizhou Provincial Key Laboratory of Pharmaceuticals, Guizhou Medical University, Guiyang, 550004, China

ARTICLE INFO

Handling editor: Professor Aiqian Ye

Keywords:

Anti-tyrosinase

Anti-browning

Aromatic aldehydes

ABSTRACT

Kojic acid-aromatic aldehydes **6a-6m** were synthesized and screened for their anti-tyrosinase activities. These compounds showed potently anti-tyrosinase activity with IC_{50} values in the range of 5.32 ± 0.23 to $77.89 \pm 3.36 \mu\text{M}$ compared with kojic acid ($IC_{50} = 48.05 \pm 3.28 \mu\text{M}$). Thereinto, compound **6j** with 3-fluorine and 4-aldehyde substitutions showed the most potent anti-tyrosinase activity ($IC_{50} = 5.32 \pm 0.23 \mu\text{M}$). Enzyme kinetic study revealed that **6j** is a noncompetitive tyrosinase inhibitor ($K_i = 2.73 \mu\text{M}$). The action mechanism of **6j** was evaluated by fluorescence spectrum quenching, molecular docking, ^1H NMR titration, etc. The anti-browning assay showed that **6j** could delay the enzymatic browning of fresh-cut apples. Besides, the cell viability assay proved that **6j** had a good safety profile as an anti-browning agent. Hence, these results identify a new class of anti-tyrosinase and anti-browning agents for further investigation in the food industry.

1. Introduction

Tyrosinase (EC 1.14.18.1), also known as polyphenol oxidase (PPO), is a copper-containing multifunctional enzyme with two copper ions at its catalytic center, which is present in several plants, microorganisms, fungi, and animals (Masum et al., 2019; Seo et al., 2003). It is a key rate-limiting enzyme participating in melanin biosynthesis, converting substrate L-tyrosine and L-DOPA to *o*-dopaquinone (Loizzo et al., 2012; Peng et al., 2022). The catalytic product *o*-quinone is transformed into melanin through a series of reactions, which can lead to the enzymatic browning of some fruits, vegetables, and aquatic products (Zhu et al., 2022). In addition, the browning of food products will lead to color and flavor changes, quality decline, loss of nutrients, low consumer acceptability, and ultimately lead to food waste (He et al., 2021; Xu et al., 2022). Therefore, tyrosinase plays an important role in the field of food preservation (especially fruits and vegetables), and can be regarded as a research target for new anti-browning agents (Yu and Fan, 2021).

Over the past few decades, many tyrosinase inhibitors were extensively discussed in the literature, but only a few of them have acceptable potency and safety and are suitable for practical applications in the food industry (He et al., 2021; Peng et al., 2022). Hence, it is urgent to

develop novel, safe and potent small molecules with anti-tyrosinase and anti-browning activity for food preservation. Among all of the reported tyrosinase inhibitors, kojic acid is a well-known one, which is derived from secondary fungal metabolites (such as *Aspergillus* spp. and *Penicillium* spp.) and can inhibit tyrosinase activity and delay the enzymatic browning of the fresh food preservation (Wu et al., 2019). For example, kojic acid combined with L-cysteine and 4-hexylresorcinol displayed a potent anti-browning effect on apple juice (Iyidogan and Bayindirli, 2004). Kojic acid also can inhibit pericarp browning by maintaining antioxidant enzyme activity during the pre-storage application of litchi fruit (Shah et al., 2017). Because kojic acid has potential application as a food anti-browning agent, and the hydroxylpyranone moiety of its chemical structure can chelate with the copper ions in the active site of tyrosinase, which is the main active group to inhibit the activity of tyrosinase. Therefore, structural modification and optimization of kojic acid to improve its inhibition potency of tyrosinase is an important method for developing more potent tyrosinase inhibitors (He et al., 2021). On the other hand, many aromatic aldehydes have been reported to be tyrosinase inhibitors and exhibited potent tyrosinase inhibitory activity in the past decade, such as 4-hydroxybenzaldehyde, cuminaldehyde, anisaldehyde, etc., indicating that they can be used as a

* Corresponding author. College of Food Science and Technology, Shanghai Ocean University, Shanghai, 201306, China.

** Corresponding author.

E-mail addresses: wj2010@126.com (J.J. Wang), yzhao@shou.edu.cn (Y. Zhao).

<https://doi.org/10.1016/j.crfs.2022.100421>

Received 20 November 2022; Received in revised form 14 December 2022; Accepted 19 December 2022

Available online 22 December 2022

2665-9271/© 2022 The Authors. Published by Elsevier B.V. This is an open access article under the CC BY-NC-ND license (<http://creativecommons.org/licenses/by-nc-nd/4.0/>).

privileged scaffold to develop new tyrosinase inhibitors (Ashraf et al., 2015; Zoighadri et al., 2019).

Molecular hybridization is a strategy to design new bioactive compounds based on the recognition of pharmacophoric fragments in a known bioactive molecules (Shaveta et al., 2016). It often combines two or more bioactive pharmacophores with similar biological activity into one molecule, and finally builds a new molecular structure with a high activity. Inspired by the above-mentioned findings and our previous work in developing novel tyrosinase inhibitors, a class of kojic acid-aromatic aldehydes **6a-6m**, combined structures of aromatic aldehyde and kojic acid, were synthesized and screened for their *in vitro* anti-tyrosinase activity (Fig. 1). All the newly synthesized compounds (**6a-6m**) were screened for their *in vitro* tyrosinase inhibitory activity. Besides, the inhibition mechanism, anti-browning effects, and cell viability of the most potent compound **6j** were also investigated.

2. Materials and methods

2.1. Materials

The nuclear magnetic resonance spectra (^1H NMR and ^{13}C NMR) were recorded with a 400 MHz JNM spectrometer (JEOL Ltd., Japan) in DMSO- d_6 as solvent and tetramethylsilane (TMS) as an external reference. The high-resolution mass spectra (HRMS) were recorded with a MicroQTOFII Bruker mass spectrometer on ESI $^-$ mode. All reagents were purchased commercially and without further purification.

2.2. Preparation of compounds 6a-6m

2.2.1. 2-(Hydroxymethyl)-5-((4-methoxybenzyl)oxy)-4H-pyran-4-one (**2**)

A mixture of **1** (35 mmol), K_2CO_3 (42 mmol), PMBCl (38.7 mmol), and DMF (30 mL) was stirred at 80 °C for 6 h. After the completed reaction, the reaction mixture was poured into 300 mL of water and the resulting precipitate was collected by filtration. The crude product was further purified by silica gel chromatography (petroleum ether/ethyl acetate, yield = 55%).

2.2.2. 2-(Chloromethyl)-5-((4-methoxybenzyl)oxy)-4H-pyran-4-one (**3**)

A mixture of **2** (5 mmol), Et_3N (1.5 mmol), tosyl chloride (7.5 mmol), and DMAP (7.5 mmol) in CH_2Cl_2 (100 mL) was stirred at room temperature for 12 h. Then, the reaction mixture was washed with diluted HCl solution and brine, dried over Na_2SO_4 , and evaporated. The residue was purified by silica gel chromatography (petroleum ether/ethyl acetate) to give product **3** (yield = 76%).

2.2.3. General procedures for the synthesis of 5a-5m

A mixture of **3** (1 mmol), K_2CO_3 (3 mmol), KI (1 mmol), and different substituted hydroxybenzaldehydes **4a-4m** (1.5 mmol) in 10 mL acetone was stirred at room temperature for 6 h. After completion (as indicated

by TLC-monitoring), the mixture was filtrated and the solvent was removed by evaporation under a reduced pressure. The residue was purified by chromatography (petroleum ether/ethyl acetate) to give the products **5a-5m**.

2.2.4. General procedures for the synthesis of 6a-6m

Compound **5** (1 mmol), trifluoroacetic acid (3 mL), and CH_2Cl_2 (10 mL) were placed in a round-bottom flask and stirred at 25 °C for 3 h. The mixture was evaporated in vacuo and the residue was purified by chromatography (petroleum ether/ethyl acetate) to give the title compounds **6a-6m**.

2.3. Anti-tyrosinase activity and kinetic analysis

In this experiment, the anti-tyrosinase activity of compounds **6a-6m** was evaluated according to our previously published protocol with kojic acid as the positive control (Peng et al., 2022). The stock solution of the tested samples was prepared with DMSO and diluted with PBS. A series of L-DOPA solutions (0.125–2 mM) and selected compound **6j** (0.0, 0.5, 1.5, and 2.0 μM) were used to research the enzyme kinetic mechanism. The inhibition type and inhibition constant (K_i) of inhibitor were determined through Lineweaver-Burk plots and secondary replot of $1/V$ against different concentrations of inhibitor, respectively.

2.4. Fluorescence spectrum quenching

Added different concentrations of inhibitor solution (2.5 μL) to tyrosinase solution (200 U/mL, 1.5 mL) (Peng et al., 2021). After equilibrating the mixture (room temperature, 5 min), the fluorescence intensity was recorded by Hitachi's spectrofluorophotometer (F-7100) with emission wavelengths (290–450 nm), emission slit width (5 nm), and excitation wavelength (280 nm).

2.5. ANS-binding fluorescence spectrum quenching

The same volume of ANS (8-anilino-1-naphthalene sulfonate) solution (80 μM) and tyrosinase solution (400 U/mL) were mixed and incubated at 25 °C for 0.5 h (Chai et al., 2019). Then, added 2.5 μL tyrosinase inhibitor solution (different concentrations) and scanned fluorescence with a spectrofluorophotometer with emission wavelengths (400–600 nm), emission slit width (5 nm), and excitation wavelength (390 nm).

2.6. Molecular docking study

According to our previous work, the molecular docking experiment was performed by Autodock vina 1.1.2 (Peng et al., 2022). The 3D structure of tyrosinase (2Y9X) and the compound were downloaded from PDB (www.rcsb.org) and drawn by ChemBio3D Ultra 14.0,

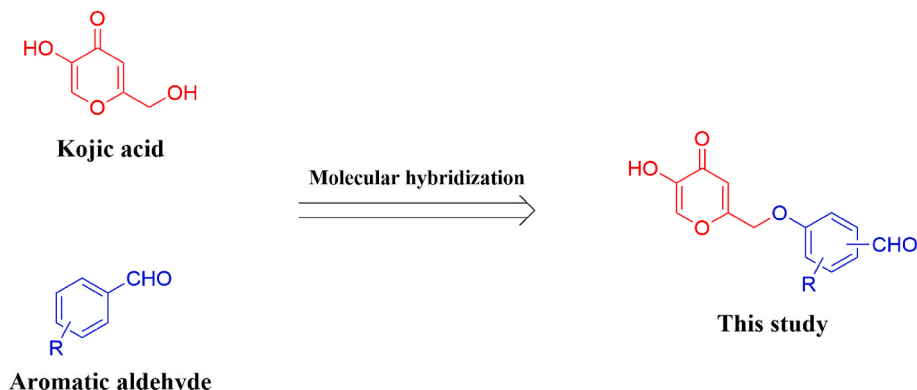


Fig. 1. Rationale design of the title compounds of this study.

respectively. The docking input files were prepared by using an AutoDockTools 1.5.6 package. The compound was prepared by merging non-polar hydrogen atoms and defining rotatable bonds. The binding pocket was determined according to the position of the original ligands ($x = -10.044$, $y = -28.706$, $z = -43.443$, and $\text{radius} = 15$). The value of exhaustiveness was fixed at 16. The docking results were analyzed and visualized with PyMol 1.7.6.

2.7. ^1H NMR titration

A solution of compound **6j** (0.6 mL, 15 mM) in DMSO- d_6 was prepared, and then added 60 μL tyrosinase solution (50 mg/mL) or 60 μL distilled water (Xie et al., 2016). After equilibration for 5 min, the ^1H NMR spectra were determined by using nuclear magnetic resonance spectra (JNM spectrometer).

2.8. Anti-browning experiment

Fresh-cut apples were used as a model to investigate the anti-browning effect of compound **6j** and kojic acid (positive control). The fresh-cut apple slices were dipped into the solution of compound **6j** for 5 min and then stored at 4 $^\circ\text{C}$ in a refrigerator. The color changes (a^* , L^* , and b^*) of the model were determined daily with an NR20XE Precision Colorimeter (Chen et al., 2021). The distilled water treatment group was used as the negative control. The color measurement was repeated 6 times for each sample. The value of ΔE was obtained as follows:

$$\Delta E = \left[(L_t^* - L_{\text{initial}}^*)^2 + (a_t^* - a_{\text{initial}}^*)^2 + (b_t^* - b_{\text{initial}}^*)^2 \right]^{0.5}$$

2.9. Cell viability assay

The normal cell line HEK-293 (1×10^5 cells/well) was seeded and incubated in 96-well plates at 37 $^\circ\text{C}$ for 24 h (Fan et al., 2023). Then, added the solutions of compound **6j** and further incubated for another 24 h. Finally, 10 μL CCK-8 solution was added and incubate for another 2 h. The cell viability was determined by BIO-RAD 680 ELISA reader (450 nm). The experiments were repeated 3 times for each sample.

3. Results and discussion

3.1. Preparation of compounds 6a-6m

The synthesis route of kojic acid-aromatic aldehydes **6a-6m** is shown in Fig. 2. The reaction between commercially available kojic acid **1** and para-methoxybenzyl (PMBCl) generated PMB-protected kojic acid **2** in the catalyst of K_2CO_3 . Intermediate product **2** was reacted with tosyl chloride (TsCl) to produce compound **3**. Condensation of **3** with appropriately substituted hydroxybenzaldehydes **4a-4m** generated the key intermediates (**5a-5m**) in the presence of K_2CO_3 and KI. Finally, the PMB-protecting group of intermediates **5a-5m** was removed with TFA to produce title compounds **6a-6m**. All the chemical structures of kojic acid-aromatic aldehydes **6a-6m** were confirmed by ^1H NMR, ^{13}C NMR, and HRMS (see Supplementary Material, Figs. S1–S39), and these compounds were new compounds that were never reported in the literature.

3.2. Structural characterization

The molecular formula of **6j** was determined as $\text{C}_{13}\text{H}_9\text{FO}_5$ by the molecular ion peak (m/z 263.0363) in HRMS (Xu et al., 2021). The ^1H NMR spectrum of **6j** (Fig. S28 and Table S1) showed a singlet signal for the OCH_2 at δ 5.17 ppm (s, 2H, H-7). The CH protons of the hydroxypyranone ring showed two singlets at δ 8.14 ppm (s, 1H, H-1') and δ 6.61 ppm (s, 1H, H-4'). A singlet signal of the hydroxyl proton in the hydroxypyranone ring appeared at δ 9.32 ppm (s, 1H, OH-C-2'). The phenyl protons showed two doublet doublets (dd) with each at δ 7.06 ppm (dd, 1H, phenyl-H-6) and δ 7.16 ppm (dd, 1H, phenyl-H-2), and a triplet at δ 7.82 ppm (t, 1H, phenyl-H-5), respectively. The proton of the aldehyde group (CHO) exhibited a singlet signal at δ 10.09 ppm (s, 1H, CHO-C-4). In the ^{13}C NMR spectrum of **6j** (Fig. S29 and Table S1), the carbon of methylene appeared a signal at δ 66.56 ppm (C-7). The signals at δ 174.10 ppm (C-3') and 186.80 ppm (CHO-C-4) were attributed to the carbonyl carbons of hydroxypyranone and aldehyde moiety, respectively. The carbon signal of C-3 was shown doublet peak at δ 164.42 ppm ($J = 170.6$ Hz) owing to $^1J_{\text{CF}}$. Besides, there were 9 carbon signals at δ 103.26 (C-2), 112.67 (C-6), 113.42 (C-4'), 118.46 (C-4), 131.47 (C-5), 140.54 (C-1'), 146.59 (C-2'), 161.66 (C-5'), and 164.20 (C-1).

The HMBC correlations (Table S2, Figs. S40–S43) derived from the

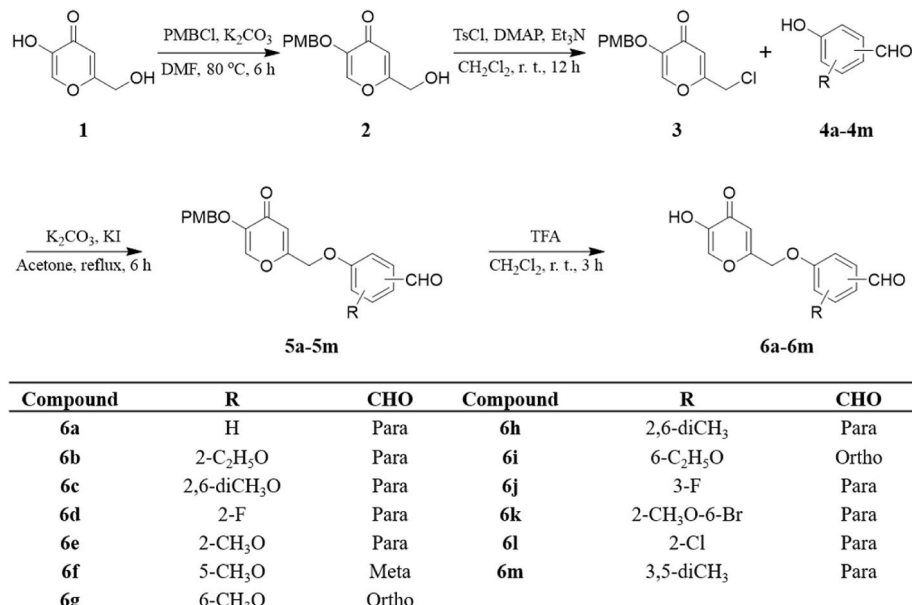


Fig. 2. Synthesis pathway of kojic acid-aromatic aldehydes.

protons at δ 7.16 (H-2) to C-1, C-3, C-4 and C-6, from δ 7.82 (H-4) to C-1, C-4 and CHO-C4, from δ 7.06 (H-5) to C-1, C-2 and C-4 indicated that the compound structure contains a phenyl moiety. The correlations from δ 6.61 (H-1') to C-2', C-3', and C-5', from δ 8.14 (H-4') to C-2', C-3', C-5', and C-7 indicated that the presence of hydroxypyranone structure in the compound structure. In addition, the correlations from δ 7.82 (H-4) to CHO-C4, and from δ 10.09 (CHO-C4) to C-5 showed that CHO was connected to the C-4 position of the phenyl. The δ 9.32 (HO-C2') correlated with C-1', C-2', and C-3', indicating that OH was located at the 2'-position of the pyranone ring. Furthermore, the key HMBC correlations between δ 5.17 (H-7) and C-4', C-5', and C-1 showed that the phenyl and hydroxypyranone were linked by CH₂O. Therefore, these spectral data confirmed the proposed chemical structure of compound **6j** (Fig. S43).

3.3. Tyrosinase inhibitory activity

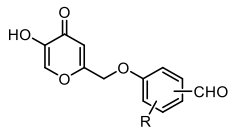
All the newly synthesized kojic acid-aromatic aldehydes (**6a-6m**) were screened for their *in vitro* anti-tyrosinase activity. These compounds showed potently anti-tyrosinase activity with IC₅₀ values ranging from 5.32 ± 0.23 to 77.89 ± 3.36 μ M when compared to kojic acid (IC₅₀ = 48.05 ± 3.28 μ M) (Table 1). Among them, compounds **6a**, **6d**, and **6j** showed potent anti-tyrosinase activities with IC₅₀ values being 5.98 ± 0.79 μ M, 9.78 ± 1.59 μ M, and 5.32 ± 0.23 μ M, respectively. Compounds **6b**, **6e**, **6f**, **6l**, and **6m** displayed moderate tyrosinase inhibitory activities with IC₅₀ values being 37.34 ± 1.76 μ M, 26.44 ± 0.26 μ M, 25.31 ± 3.11 μ M, 12.75 ± 0.58 μ M, and 12.39 ± 1.22 μ M. Other compounds (**6c**, **6g**, **6h**, **6i**, and **6k**) displayed relatively lower inhibitory activity against tyrosinase. In this series, compound **6j**, containing 3-F and 4-aldehyde substitutes, showed the most potent anti-tyrosinase activity, with nine folds more active than the positive control (kojic acid, IC₅₀ = 48.05 ± 3.28 μ M).

3.4. Structure-activity relationship (SAR)

The SAR of kojic acid-aromatic aldehydes **6a-6m** has been summarized in Fig. 3. By comparing the inhibitory activities of compounds **6g** (ortho position), **6i** (ortho position), and **6f** (meta position) with other compounds (para position), it can be found that the position of the aldehyde group in the structure presented a great influence on their activity. The effect of the position of the aldehyde group on the activity

Table 1

Anti-tyrosinase activities of kojic acid-aromatic aldehydes (**6a-6m**) and kojic acid.



Compounds	R	CHO	IC ₅₀ (μ M)
6a	H	Para	5.98 ± 0.79
6b	2-C ₂ H ₅ O	Para	37.34 ± 1.76
6c	2,6-diCH ₃ O	Para	>100
6d	2-F	Para	9.78 ± 1.59
6e	2-CH ₃ O	Para	26.44 ± 0.26
6f	5-CH ₃ O	Meta	25.31 ± 3.11
6g	6-CH ₃ O	Ortho	>100
6h	2,6-diCH ₃	Para	77.18 ± 4.34
6i	6-C ₂ H ₅ O	Ortho	>100
6j	3-F	Para	5.32 ± 0.23
6k	2-CH ₃ O-6-Br	Para	77.89 ± 3.36
6l	2-Cl	Para	12.75 ± 0.58
6m	3,5-diCH ₃	Para	12.39 ± 1.22
Kojic acid			48.05 ± 3.28

could be ranked as para position > meta position > ortho position. The reason was probably that when the aldehyde group was in para-position, the compound presented a linear structure and was easier to enter the long and narrow cavity near the active binding site to inhibit tyrosinase catalytic activity (Liu et al., 2008). The simultaneous introduction of substituents into the two ortho-positions (2- and 6- positions) of the hydroxypyranone structure resulted in the decrease of the inhibitory activity (**6c** and **6k**), possibly owing to the large steric hindrance of molecular structure which prevented compound from entering the long and narrow cavity. Comparing the inhibitory activity of **6a** (5.98 ± 0.79 μ M) with **6b** (37.34 ± 1.76 μ M), **6e** (26.44 ± 0.26 μ M), **6l** (12.75 ± 0.58 μ M), and **6m** (12.39 ± 1.22 μ M), the result was shown that introduction of larger substituents into the phenyl significantly decreased inhibitory activity. Interestingly, the introduction of smaller fluorine into the phenyl ring resulted in a slight decrease (**6d**) or increase (**6j**) in biological activity. In particular, compound **6j** with 3-fluorine and 4-aldehyde substitutions showed the most potent anti-tyrosinase activity. Hence, these identified SARs had a great potential to be optimized to produce more potent tyrosinase inhibitors. In fact, the hydroxypyranone moiety is the key active pharmacophore of kojic acid, and therefore, the combination of this moiety with other pharmacophores is the main method to prepare new tyrosinase inhibitors (He et al., 2021). Aromatic aldehyde exists in many foods and it is a pharmacophore of tyrosinase inhibitor (Zolghadri et al., 2019). Therefore, we chose the combination of food-derived aromatic aldehyde and hydroxypyranone to prepare new tyrosinase inhibitors in this study. In addition, diet-derived flavonoids are also one of the important active ingredients in food, and they have a variety of activities such as anti tyrosinase, anti-oxidation, anti-bacterial ability, etc (Lyu et al., 2022; Teng et al., 2023; Teng et al., 2022; Teng et al., 2021). In the future, the preparation of kojic acid derivatives containing diet-derived flavonoids may become new and safe anti-browning agents.

3.5. Kinetic analysis

To study the tyrosinase inhibition mechanism of kojic acid-aromatic aldehydes **6a-6m**, the most potent compound **6j** was chosen as a representative for the enzyme kinetic study. The reaction rates of tyrosinase were measured in the presence of inhibitor **6j** (0.0, 0.5, 1.5, and 2.0 μ M) and the substrate of L-DOPA (0.125–2 mM). As shown in Lineweaver-Burk plots (Fig. 4A), V_{max} values were gradually decreased with the increase of tyrosinase inhibitor **6j** but K_m values did not change, indicating that **6j** was a non-competitive tyrosinase inhibitor (Şöhretoğlu et al., 2018). On the other hand, the secondary re-plots of Lineweaver-Burk plots were performed to calculate the K_i value of compound **6j** (Fig. 4B). Based on these facts, it is reasonably believed that **6j** is a noncompetitive inhibitor against tyrosinase (K_i = 2.73 μ M).

3.6. Fluorescence spectrum quenching

Due to the presence of some amino acid residues such as phenylalanine (Phe), tryptophan (Trp), and tyrosine (Tyr) as fluorophores, proteins or enzymes can exhibit intrinsic fluorescence under specific excitation light sources (Roy, 2017). When small molecule inhibitors interact with the active binding site of the enzymes, the microenvironment of fluorophores of the enzymes will change, leading to changes in the fluorescence intensity. Hence, the fluorescence technique is an important method in the research of interaction mechanisms between small molecule inhibitors and enzymes (Zhao et al., 2017).

To explore the interaction mechanism of compound **6j** with tyrosinase, the fluorescence intensity of tyrosinase was determined in the absence and presence of different concentrations of compound **6j** (4.99 μ M, 9.97 μ M, 14.93 μ M, 19.87 μ M, and 24.79 μ M). As shown in Fig. 5A and B, in the absence of inhibitors (the concentration of compound **6j** is 0 μ M), tyrosinase solution exhibits high fluorescence emission at 280 nm excitation wavelength, with a maximum peak of 338 nm. With the

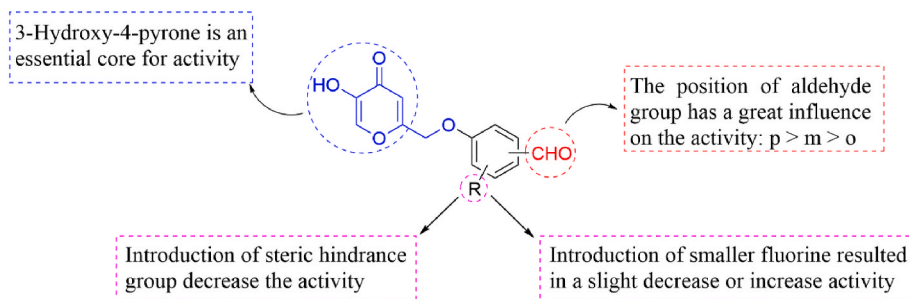


Fig. 3. Summarized SARs of kojic acid-aromatic aldehydes.

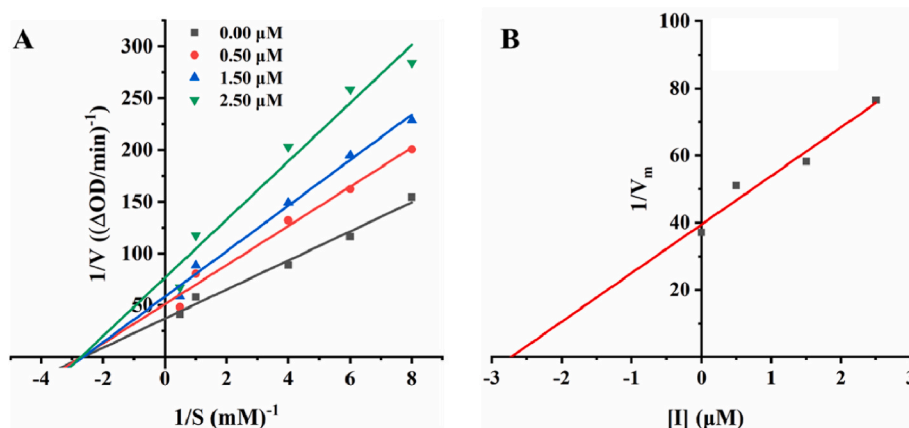


Fig. 4. Determination of the inhibition type and inhibition constant of compound 6j against tyrosinase. (A) Lineweaver-Burk plots of 6j; (B) Secondary plots of $1/V_m$ vs various concentrations of 6j.

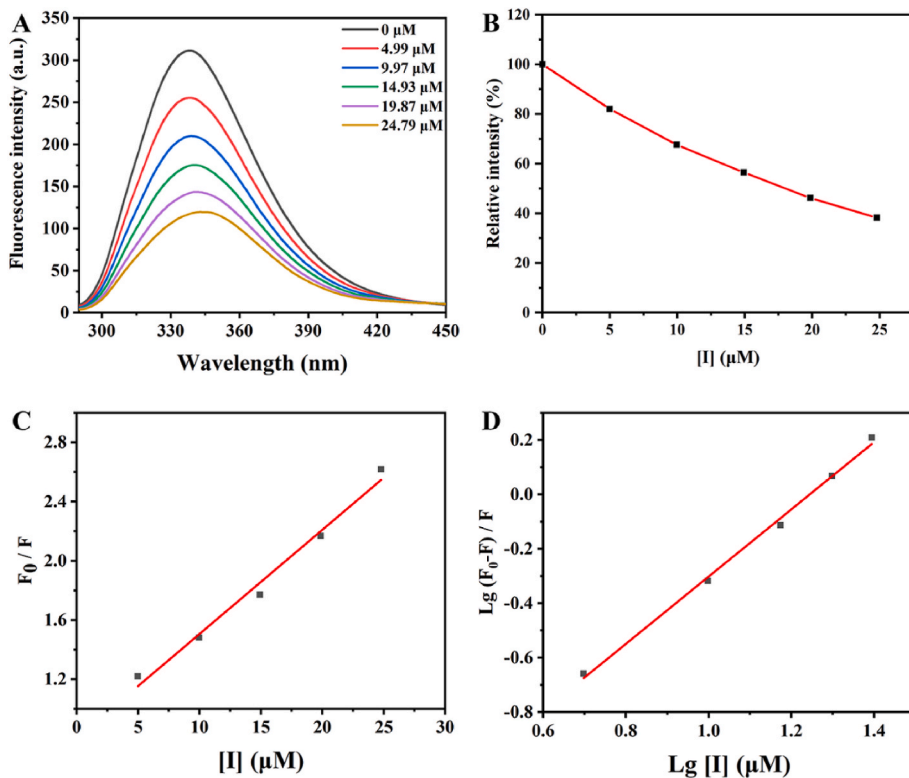


Fig. 5. The effects of compound 6j on fluorescence quenching. (A) Fluorescence emission spectra of mushroom tyrosinase in the presence of different concentration of compound 6j. (B) Relative intensity at different concentrations of compound 6j. (C) Stern-Volmer plot for the fluorescence quenching of tyrosinase; (D) Plot of $Lg(F_0 - F)/F$ against $Lg[6j]$.

increasing concentration of compound **6j** (4.99 μM , 9.97 μM , 14.93 μM , 19.87 μM , and 24.79), the fluorescence intensity of tyrosinase showed an obvious fluorescence quenching effect, which suggested that compound **6j** could bind to tyrosinase. In addition, the fluorescence quenching induced by compound **6j** was accompanied by a slight shift of the maximum emission wavelength, indicating that the microenvironment around the tyrosinase fluorescent fluorophores has changed (Zeng et al., 2020). Hence, the fluorescence spectrum quenching assay clearly suggested that compound **6j** could interact with the binding active site of tyrosinase and cause a conformational change in tyrosinase (Chen et al., 2019).

The fluorescence spectrum quenching mechanism can be divided into dynamic quenching and static quenching, and the corresponding quenching mechanism can be distinguished by analyzing the fluorescence data with the Stern-Volmer equation (He et al., 2014). As calculated in the Stern-Volmer equation, the values of K_{SV} and K_q were $7.04 \times 10^3 \text{ M}^{-1}$ and $7.04 \times 10^{11} \text{ M}^{-1} \text{ s}^{-1}$, respectively (Fig. 5C and D, Table 2) (Makarska-Bialokoz, 2018). Besides, the calculated K_q value was greater than the maximal diffusion rate constant ($2.0 \times 10^{10} \text{ Lmol}^{-1} \text{ s}^{-1}$), which indicated that the fluorescence quenching mechanism of compound **6j** with tyrosinase was a static quenching procedure (He et al., 2021). The stern-Volmer equation is as follows:

$$F_0 / F = 1 + K_q \tau_0 [Q] = 1 + K_{SV} [Q]$$

F_0 : Fluorescence intensities before add quencher; $[Q]$: Quencher concentration; F : Fluorescence intensities after add quencher; K_q : Biomolecular quenching constant; K_{SV} : Stern-Volmer quenching constant; τ_0 : 10^{-8} s

Due to the fluorescence quenching mechanism tyrosinase by compound **6j** being static, the Lineweaver-Burk equation was used to calculate the binding constant (K_a) and binding sites (n) as $2.89 \times 10^4 \text{ M}^{-1}$ and 1.24, respectively. Based on the value of n (1.24), indicates that the interaction binding site between compound **6j** and tyrosinase is only one (Joksimovic et al., 2021). The Lineweaver-Burk equation is as follows:

$$\text{Lg}[(F_0 - F) / F] = \text{Lg}K_a + n \text{Lg}[Q]$$

3.7. ANS-binding fluorescence quenching

ANS is a widely used fluorescent probe in the protein field, and when it binds with hydrophobic amino acid residues on tyrosinase, it will cause a significant increase in fluorescence intensity. Hence, ANS-binding fluorescence spectra have emerged as a valuable monitor to study the change of hydrophobic surfaces of tyrosinase mediated by inhibitors. (Zhao et al., 2020). In this study, the intensities of the ANS-binding fluorescence spectrum were recorded at the different concentrations of compound **6j**. The results were shown in Fig. 6, the maximum emission peak wavelength and intensity of ANS-binding fluorescence spectra did not present an obvious change with an increase in the concentration of compound **6j** (0 μM , 9.98 μM , 19.93 μM , 29.85 μM , 39.74 μM , 49.59 μM , and 59.41 μM). The described phenomenon suggested that compound **6j** could bind to the active site of tyrosinase and not induce the change of the hydrophobic domain (Tang et al., 2020).

Table 2

Fluorescence parameters for the interaction between quencher (**6j**) and tyrosinase.

Compound	Type of quenching	$K_{sv} (\text{M}^{-1})$	$K_q (\text{M}^{-1} \text{s}^{-1})$	$K_a (\text{M}^{-1})$	n
6j	Static	7.04×10^3	7.04×10^{11}	2.89×10^4	1.24

3.8. Molecular docking analysis

To predict the binding conformation and binding modes of compound **6j** with tyrosinase, molecular modeling was applied by AutoDock 1.1.2 (Trott and Olson, 2010). As shown in Fig. 7, compound **6j** binds to the hydrophobic cavity of tyrosinase in a compact conformation (binding energy: $-6.6 \text{ kcal mol}^{-1}$), where the hydroxypyranone moiety of compound **6j** was oriented towards copper ions. Notably, the hydroxypyranone moiety of compound **6j** can form two strong chelating bonds with copper ions (bond lengths: 2.7 and 3.0 \AA), which are the major forces between compound **6j** and tyrosinase. This result is consistent with that reported in the previous literature, which confirms that the hydroxypyranone moiety is the main structure of these compounds to play a potent anti-tyrosinase activity (Ashooriha et al., 2019). Furthermore, **6j** can form strong hydrophobic binding interaction with residues Phe-264, Met-280, Val-283, Pro-284, and Ala-286. The phenyl moiety of compound **6j** and Phe-264 formed CH- π stacking interaction. In addition, compound **6j** also formed an H bond with Val-283 (bond length: 2.7 \AA), which is another major force between compound **6j** and tyrosinase. The above molecular docking analysis gives us a clear explanation for the binding mechanism of **6j** with tyrosinase.

3.9. ^1H NMR titration

^1H NMR titration is an important tool to study the interaction mechanism of small molecular compounds with enzyme proteins. Its principle is to detect the changes in hydrogen chemical shifts of small molecular compounds before and after interacting with enzyme proteins (Liu et al., 2015; Xie et al., 2016). The interactions between compound **6j** and tyrosinase were further determined by ^1H NMR titration assay in DMSO- d_6 (Fig. 8). After adding the tyrosinase solution, the singlet signal at δ 9.25 ppm completely disappeared, indicating that the hydroxyl of compound **6j** interacted with the copper ions to form a chelate bond and the hydrogen proton was removed (Xie et al., 2016). Clearly, the ^1H NMR titration result was consistent with molecular docking, confirming that the hydroxyl group of compound **6j** was the key group that interacted with the copper ions in the active binding site of tyrosinase.

3.10. Anti-browning experiment

The enzymatic browning reaction catalyzed by tyrosinase is one of the common reasons for browning in the preservation of fruits and vegetables (Moon et al., 2020). Therefore, inhibition of enzymatic browning reaction by tyrosinase inhibitors can control browning and prolong the shelf life of foods (Zhu et al., 2022). In order to study whether compound **6j** had an anti-browning effect in real food, fresh-cut apple slices were selected to evaluate its anti-browning and preservation effect. Generally, L^* , a^* , b^* , and ΔE are the main parameters to evaluate the degree of browning (Castaner et al., 1999; Peng et al., 2021). Thereinto, the L^* value is sensitive to browning change, which is an important indicator to monitor the browning degree of foods (Hou et al., 2014). In Fig. 9A, the L^* value of all sample groups was almost the same at 0 day, but it gradually decreased with the extension of preservation days, which proved that browning happened in these samples. By comparing the changing trend of the L^* value, it can be seen that among these sample groups, **6j** treated group showed a stronger anti-browning effect than kojic acid. Besides, ΔE values and the appearance of photos also exhibited the same trend (Fig. 9B). These results are consistent with the change in the visual assessment (Fig. 9C). Hence, this study confirmed that compound **6j** displays potent tyrosinase inhibitory activity and anti-browning effects, which could be considered as an anti-browning agent for further investigation. It must be pointed out that the enzymatic browning reaction of fresh fruits and vegetables is related to many factors, such as the activities of PPO (tyrosinase), POD, and PAL, and the content of total polyphenols (Liu et al., 2019; Shao et al., 2018). Anti-browning agents in food industries may inhibit enzymatic

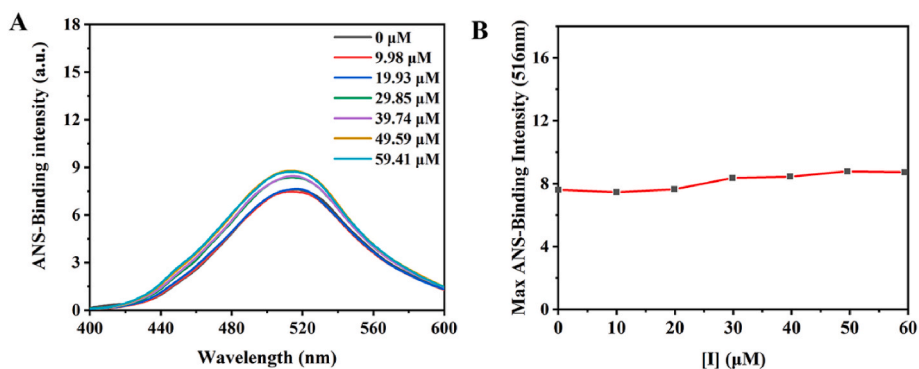


Fig. 6. ANS-binding fluorescence spectra of tyrosinase with different concentrations of compound **6j**. (A) ANS-binding intensity of tyrosinase with the different concentrations of compound **6j**. (B) Maximum ANS-fluorescence intensity of tyrosinase in the presence of different concentrations of compound **6j**.

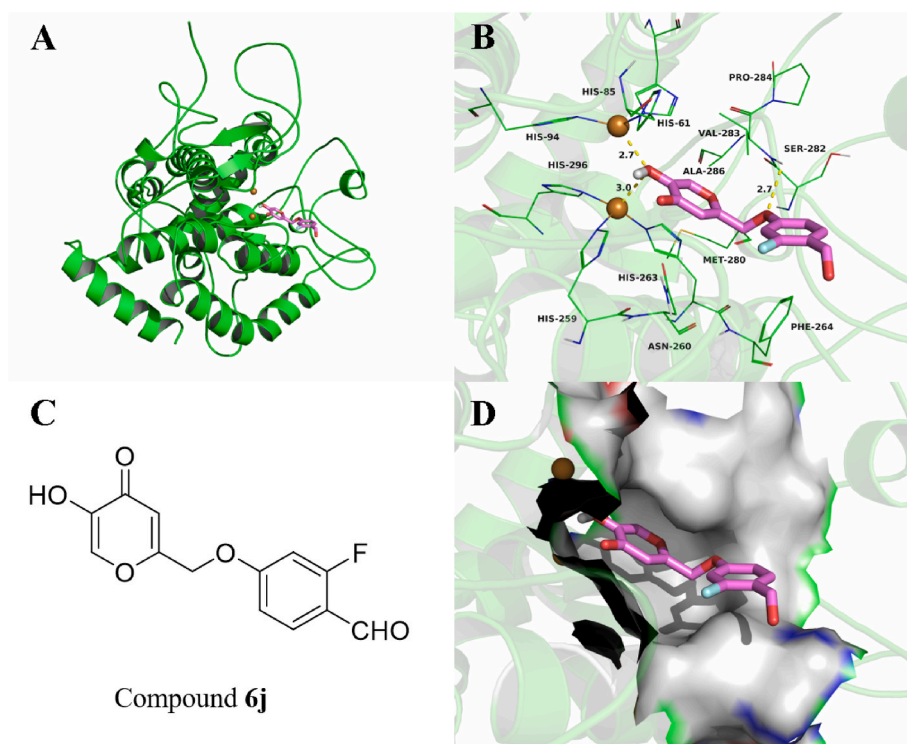


Fig. 7. Binding pose of compound **6j** in the binding site of the tyrosinase. (A) The overall structure of tyrosinase with **6j**; (B) Binding pose of **6j** in the binding site; (C) Chemical structure of **6j**; (D) Binding pose of **6j** in the surface of the binding pocket.

browning reactions by acting on one or more of these factors, and play a role in controlling the browning process and extending the shelf life of fresh fruits and vegetables (Liu et al., 2019; Zhu et al., 2022). Our study preliminarily confirmed the inhibitory effect of compound **6j** on tyrosinase activity and food browning, but its in-depth anti-browning mechanism needs to be further studied in the future.

3.11. Cell viability evaluation

For the anti-browning agents used in the food industry, safety is a very important inspection index. To evaluate the safety of compound **6j** as a food anti-browning agent, a cell viability assay was performed on the human normal cell line HEK293 (Table 3). The results showed that compound **6j** did not inhibit the cell growth at the concentration of 1 μM , 4 μM , 16 μM and 64 μM supported by that all the cell survival rates reached $97.06 \pm 2.49\%$, $105.92 \pm 8.83\%$, $102.42 \pm 10.08\%$, and $105.30 \pm 7.27\%$, respectively. Even though the concentration was increased to 256 μM , compound **6j** only showed a slight inhibitory effect

on human normal cell lines with a survival rate of $88.57 \pm 3.61\%$. Due to compound **6j** can inhibit tyrosinase activity and prevent enzymatic browning of fresh food at a very low concentration (tyrosinase: $\text{IC}_{50} = 5.32 \pm 0.23 \mu\text{M}$), it is firmly proven to be safe for normal cells at the low concentration. Hence, compound **6j** was proved to be a safe anti-browning agent in the food industry and could be used as a lead compound for the development of a new anti-browning agent in the future.

4. Conclusion

A novel class of kojic acid-aromatic aldehydes **6a-6m** were designed and synthesized, and these compounds displayed potentially anti-tyrosinase activity with IC_{50} values ranging from 5.32 ± 0.23 to $77.89 \pm 3.36 \mu\text{M}$ compared with kojic acid ($\text{IC}_{50} = 48.05 \pm 3.28 \mu\text{M}$). Notably, compound **6j** with 3-fluorine and 4-aldehyde substitutions on the phenyl showed the most potent anti-tyrosinase activity. Enzyme kinetic study showed that **6j** was a non-competitive tyrosinase inhibitor, and the position of the aldehyde group and the steric hindrance of substituents

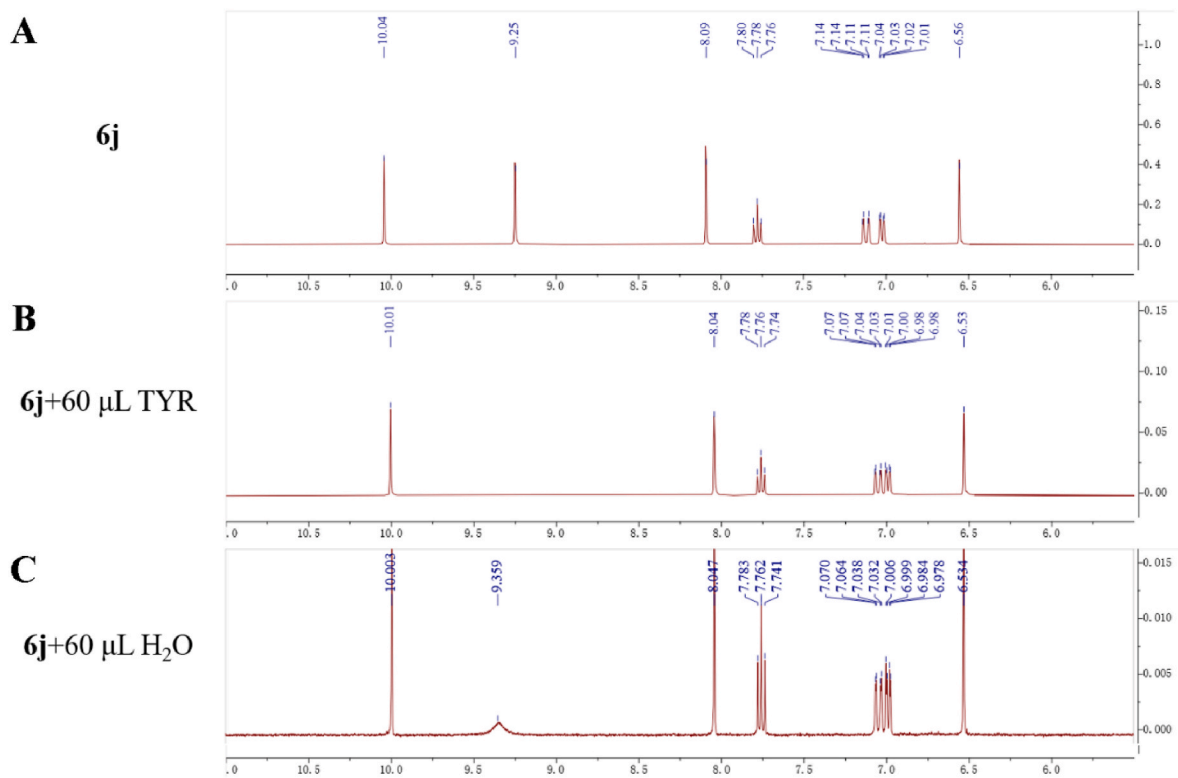


Fig. 8. ¹H NMR titration spectra of compound **6j** with tyrosinase (TYR). (A) ¹H NMR spectrum of **6j** in DMSO-d₆; (B) ¹H NMR spectrum of **6j** and 60 μL tyrosinase in DMSO-d₆; (C) ¹H NMR spectrum of **6j** and 60 μL H₂O in DMSO-d₆.

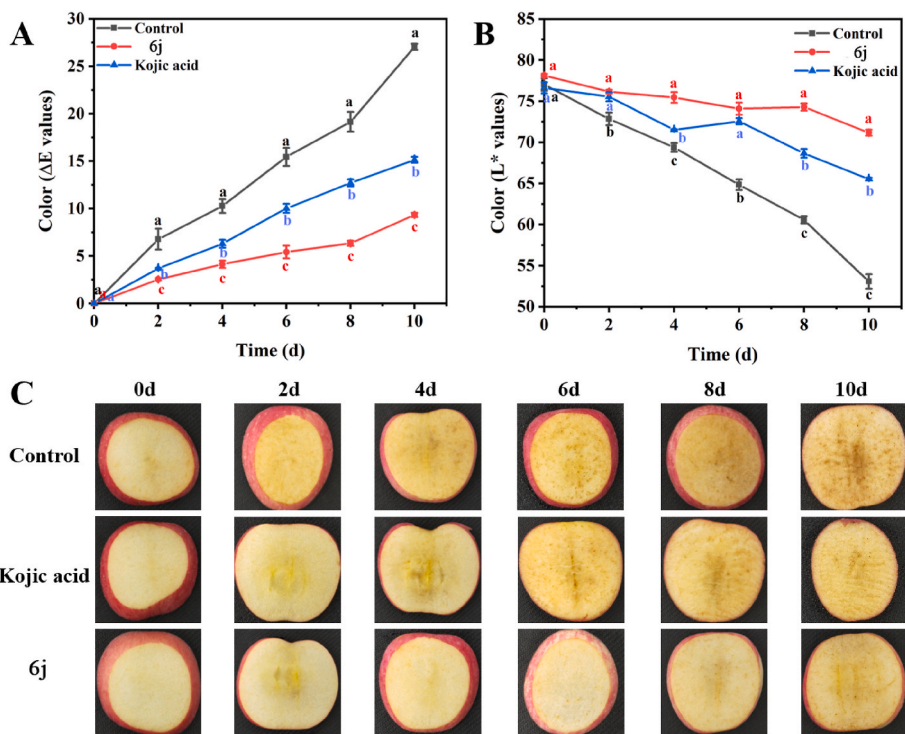


Fig. 9. Anti-browning experiments with the fresh-cut apple slices. (A) ΔE; (B) L*; (C) Photographs.

in the structure possessed a great influence on its activity. Meanwhile, compound **6j** displayed anti-tyrosinase activity by chelating with copper ions of tyrosinase. Anti-browning experiments and cell viability assay showed that compound **6j** has a good anti-browning effect on apples and

safety, respectively. Therefore, this study synthesized novel and effective tyrosinase inhibitors which displayed great potential to be regarded as anti-browning agents to preserve food quality and safety.

Table 3

Toxicity of compound **6j** against normal human embryonic kidney cells 293.

Concentration	1 μ M	4 μ M	16 μ M	64 μ M	256 μ M
Viability (%)	97.06 \pm 2.49	105.92 \pm 8.83	102.42 \pm 10.08	105.30 \pm 7.27	88.57 \pm 3.61

CRedit authorship contribution statement

Zhiyun Peng: designed the study, did the experiment and analyze the data wrote the manuscript. **Guangcheng Wang:** did the experiment, and, Formal analysis, wrote the manuscript. **Yan He:** designed the study. **Jing Jing Wang:** designed the study and revised the manuscript. **Yong Zhao:** designed the study revised the manuscript and.

Declaration of competing interest

The authors declare that they have no known competing financial interests or personal relationships that could have appeared to influence the work reported in this paper.

Data availability

The data that has been used is confidential.

Acknowledgements

This work was supported by the National Natural Science Foundation of China (32102105; 3167177); Program of Shanghai Academic Research Leader (21XD1401200); the Guangdong Basic and Applied Basic Research Foundation (2020A1515110960; 2020A1515110326; 2021A1515010015), the Discipline Construction Program of Foshan University (CGZ0400162).

Appendix A. Supplementary data

Supplementary data to this article can be found online at <https://doi.org/10.1016/j.crfs.2022.100421>.

References

- Ashoori, M., Khoshneviszadeh, M., Khoshneviszadeh, M., Moradi, S.E., Rafiei, A., Kardan, M., Emami, S., 2019. 1,2,3-Triazole-based kojic acid analogs as potent tyrosinase inhibitors: design, synthesis and biological evaluation. *Bioorg. Chem.* 82, 414–422. <https://doi.org/10.1016/j.bioorg.2018.10.069>.
- Ashraf, Z., Rafiq, M., Seo, S.Y., Babar, M.M., Zaidi, N., 2015. Synthesis, kinetic mechanism and docking studies of vanillin derivatives as inhibitors of mushroom tyrosinase. *Bioorg. Med. Chem.* 23 (17), 5870–5880. <https://doi.org/10.1016/j.bmc.2015.06.068>.
- Castaner, M., Gil, M.I., Ruiz, M.V., Artes, F., 1999. Browning susceptibility of minimally processed Baby and Romaine lettuces. *Eur. Food Res. Technol.* 209 (1), 52–56. <https://doi.org/10.1007/s002170050456>.
- Chai, W., Wei, Q., Deng, W., Zheng, Y., Chen, X., Huang, Q., Chong, O., Peng, Y., 2019. Anti-melanogenesis properties of condensed tannins from *Vigna angularis* seeds with potent antioxidant and DNA damage protection activities. *Food Funct.* 10 (1), 99–111. <https://doi.org/10.1039/c8fo01979g>.
- Chen, B., Huang, J., Liu, Y., Liu, H., Zhao, Y., Wang, J.J., 2021. Effects of the curcumin-mediated photodynamic inactivation on the quality of cooked oysters with *Vibrio parahaemolyticus* during storage at different temperature. *Int. J. Food Microbiol.* 345, 109152. <https://doi.org/10.1016/j.ijfoodmicro.2021.109152>.
- Chen, Y.M., Li, C., Zhang, W.J., Shi, Y., Wen, Z.J., Chen, Q.X., Wang, Q., 2019. Kinetic and computational molecular docking simulation study of novel kojic acid derivatives as anti-tyrosinase and antioxidant agents. *J. Enzym. Inhib. Med. Chem.* 34 (1), 990–998. <https://doi.org/10.1080/14756366.2019.1609467>.
- Fan, M., Yang, W., Peng, Z., He, Y., Wang, G., 2022. Chromone-based benzohydrazide derivatives as potential α -glucosidase inhibitor: synthesis, biological evaluation and molecular docking study. *Bioorg. Chem.* 131, 106276. <https://doi.org/10.1016/j.bioorg.2022.106276>. Forthcoming.
- He, M., Fan, M., Liu, W., Li, Y., Wang, G., 2021a. Design, synthesis, molecular modeling, and biological evaluation of novel kojic acid derivatives containing bioactive heterocycle moiety as inhibitors of tyrosinase and antibrowning agents. *Food Chem.* 362, 130241. <https://doi.org/10.1016/j.foodchem.2021.130241>.

- He, M., Fan, M., Peng, Z., Wang, G., 2021b. An overview of hydroxypyranone and hydroxypyridinone as privileged scaffolds for novel drug discovery. *Eur. J. Med. Chem.* 221, 113546. <https://doi.org/10.1016/j.ejmech.2021.113546>.
- He, Y., Jiao, B., Tang, H., 2014. Interaction of single-stranded DNA with graphene oxide: fluorescence study and its application for S1 nuclease detection. *RSC Adv.* 4 (35), 18294–18300. <https://doi.org/10.1039/c4ra01102c>.
- Hou, Z.Q., Feng, Y.Y., Wei, S.C., Wang, Q.G., 2014. Effects of curing treatment on the browning of fresh-cut potatoes. *Am. J. Potato Res.* 91 (6), 655–662. <https://doi.org/10.1007/s12230-014-9396-6>.
- Iyidogan, N.F., Bayindirli, A., 2004. Effect of L-cysteine, kojic acid and 4-hexylresorcinol combination on inhibition of enzymatic browning in Amasya apple juice. *J. Food Eng.* 62 (3), 299–304. [https://doi.org/10.1016/s0260-8774\(03\)00243-7](https://doi.org/10.1016/s0260-8774(03)00243-7).
- Joksimovic, N., Petronijevic, J., Cocic, D., Jankovic, N., Milovic, E., Kosanic, M., Petrovic, N., 2021. Synthesis, characterization, biological evaluation, BSA binding properties, density functional theory and molecular docking study of Schiff bases. *J. Mol. Struct.* 1244, 130952. <https://doi.org/10.1016/j.molstruc.2021.130952>.
- Liu, J., Yi, W., Wan, Y., Ma, L., Song, H., 2008. 1-(1-Arylethylidene)thiosemicarbazide derivatives: a new class of tyrosinase inhibitors. *Bioorg. Med. Chem.* 16 (3), 1096–1102. <https://doi.org/10.1016/j.bmc.2007.10.120>.
- Liu, X., Li, Y., Zhang, Y., Zhao, Q., Song, W., Xu, J., Bu, X., 2015. Ratiometric fluorescence detection of fluoride ion by indole-based receptor. *Talanta* 131, 597–602. <https://doi.org/10.1016/j.talanta.2014.08.017>.
- Liu, X., Yang, Q., Lu, Y., Li, Y., Li, T., Zhou, B., Qiao, L., 2019. Effect of purslane (*Portulaca oleracea* L.) extract on anti-browning of fresh-cut potato slices during storage. *Food Chem.* 283, 445–453. <https://doi.org/10.1016/j.foodchem.2019.01.058>.
- Loizzo, M.R., Tundis, R., Menichini, F., 2012. Natural and synthetic tyrosinase inhibitors as antibrowning agents: an update. *Compr. Rev. Food Sci. Food Saf.* 11 (4), 378–398. <https://doi.org/10.1111/j.1541-4337.2012.00191.x>.
- Lyu, Q., Chen, L., Lin, S., Cao, H., Teng, H., 2022. A designed self-microemulsion delivery system for dihydromyricetin and its dietary intervention effect on high-fat-diet fed mice. *Food Chem.* 390, 132954. <https://doi.org/10.1016/j.foodchem.2022.132954>.
- Makarska-Bialokoz, M., 2018. Interactions of hemin with bovine serum albumin and human hemoglobin: a fluorescence quenching study. *Spectrochim. Acta Part A Molec. Biomolec. Spectrosc.* 193, 23–32. <https://doi.org/10.1016/j.saa.2017.11.063>.
- Masum, M.N., Yamauchi, K., Mitsunaga, T., 2019. Tyrosinase inhibitors from natural and synthetic sources as skin-lightening agents. *Rev. Agric. Sci.* 7, 41–58.
- Moon, K.M., Kwon, E.B., Lee, B., Kim, C.Y., 2020. Recent trends in controlling the enzymatic browning of fruit and vegetable products. *Molecules* 25 (12), 2754. <https://doi.org/10.3390/molecules25122754>.
- Peng, Z., Wang, G., Zeng, Q.-H., Li, Y., Wu, Y., Liu, H., Wang, J.J., Zhao, Y., 2021. Synthesis, antioxidant and anti-tyrosinase activity of 1,2,4-triazole hydrazones as antibrowning agents. *Food Chem.* 341, 128265. <https://doi.org/10.1016/j.foodchem.2020.128265>.
- Peng, Z., Li, Y., Tan, L., Chen, L., Shi, Q., Zeng, Q.-H., Liu, H., Wang, J.J., Zhao, Y., 2022a. Anti-tyrosinase, antioxidant and antibacterial activities of gallic acid-benzylidenehydrazine hybrids and their application in preservation of fresh-cut apples and shrimps. *Food Chem.* 378, 132127. <https://doi.org/10.1016/j.foodchem.2022.132127>.
- Peng, Z., Wang, G., Zeng, Q.-H., Li, Y., Liu, H., Wang, J.J., Zhao, Y., 2022b. A systematic review of synthetic tyrosinase inhibitors and their structure-activity relationship. *Crit. Rev. Food Sci. Nutr.* 62 (15), 4053–4094. <https://doi.org/10.1080/10408398.2021.1871724>.
- Roy, S., 2017. An insight of binding interaction between Tryptophan, Tyrosine and Phenylalanine separately with green gold nanoparticles by fluorescence quenching method. *Optik* 138, 280–288. <https://doi.org/10.1016/j.ijleo.2017.03.057>.
- Seo, S.Y., Sharma, V.K., Sharma, N., 2003. Mushroom tyrosinase: recent prospects. *J. Agric. Food Chem.* 51 (10), 2837–2853. <https://doi.org/10.1021/jf020826f>.
- Shah, H.M.S., Khan, A.S., Ali, S., 2017. Pre-storage kojic acid application delays pericarp browning and maintains antioxidant activities of litchi fruit. *Postharvest Biol. Technol.* 132, 154–161. <https://doi.org/10.1016/j.postharvbio.2017.06.004>.
- Shao, L.L., Wang, X.L., Chen, K., Dong, X.W., Kong, L.M., Zhao, D.Y., Hider, R.C., Zhou, T., 2018. Novel hydroxypyridinone derivatives containing an oxime ether moiety: synthesis, inhibition on mushroom tyrosinase and application in anti-browning of fresh-cut apples. *Food Chem.* 242, 174–181. <https://doi.org/10.1016/j.foodchem.2017.09.054>.
- Shaveta, Mishra, S., Singh, P., 2016. Hybrid molecules: the privileged scaffolds for various pharmaceuticals. *Eur. J. Med. Chem.* 124, 500–536. <https://doi.org/10.1016/j.ejmech.2016.08.039>.
- Şöhretöglü, D., Sari, S., Barut, B., Özel, A., 2018. Tyrosinase inhibition by some flavonoids: inhibitory activity, mechanism by in vitro and in silico studies. *Bioorg. Chem.* 81, 168–174. <https://doi.org/10.1016/j.bioorg.2018.08.020>.
- Tang, H., Huang, L., Zhao, D., Sun, C., Song, P., 2020. Interaction mechanism of flavonoids on bovine serum albumin: insights from molecular property-binding affinity relationship. *Spectrochim. Acta Part A Molec. Biomolec. Spectrosc.* 239, 118519. <https://doi.org/10.1016/j.saa.2020.118519>.
- Teng, H., Deng, H., Zhang, C., Cao, H., Huang, Q., Chen, L., 2022. The role of flavonoids in mitigating food originated heterocyclic aromatic amines that concerns human wellness. *Food Sci. Hum. Wellness* 12 (4), 975–985. <https://doi.org/10.1016/j.fshw.2022.10.019>. Forthcoming.
- Teng, H., Mi, Y., Deng, H., He, Y., Wang, S., Ai, C., Cao, H., Zheng, B., Chen, L., 2022. Inhibitory effect of acylated anthocyanins on heterocyclic amines in grilled chicken breast patty and its mechanism. *Curr. Res. Food Sci.* 5, 1732–1739. <https://doi.org/10.1016/j.crfs.2022.09.011>.

- Teng, H., Zheng, Y., Cao, H., Huang, Q., Xiao, J., Chen, L., 2021. Enhancement of bioavailability and bioactivity of diet-derived flavonoids by application of nanotechnology: a review. *Crit. Rev. Food Sci. Nutr.* <https://doi.org/10.1080/10408398.2021.1947772>.
- Trott, O., Olson, A.J., 2010. Software news and update AutoDock Vina: improving the speed and accuracy of docking with a new scoring function, efficient optimization, and multithreading. *J. Comput. Chem.* 31 (2), 455–461. <https://doi.org/10.1002/jcc.21334>.
- Wu, Y., Shi, Y.-g., Zeng, L.-y., Pan, Y., Huang, X.-y., Bian, L.-q., Zhu, Y.-j., Zhang, R.-r., Zhang, J., 2019. Evaluation of antibacterial and anti-biofilm properties of kojic acid against five food-related bacteria and related subcellular mechanisms of bacterial inactivation. *Food Sci. Technol. Int.* 25 (1), 3–15. <https://doi.org/10.1177/1082013218793075>.
- Xie, J., Dong, H.H., Yu, Y.Y., Cao, S.W., 2016. Inhibitory effect of synthetic aromatic heterocycle thiosemicarbazone derivatives on mushroom tyrosinase: insights from fluorescence, ¹H NMR titration and molecular docking studies. *Food Chem.* 190, 709–716. <https://doi.org/10.1016/j.foodchem.2015.05.124>.
- Xu, H., Li, X., Mo, L., Zou, Y., Zhao, G., 2022. Tyrosinase inhibitory mechanism and the anti-browning properties of piceid and its ester. *Food Chem.* 390, 133207 <https://doi.org/10.1016/j.foodchem.2022.133207>.
- Xu, Y., Li, H., Liang, J., Ma, J., Yang, J., Zhao, X., Zhao, W., Bai, W., Zeng, X., Dong, H., 2021. High-throughput quantification of eighteen heterocyclic aromatic amines in roasted and pan-fried meat on the basis of high performance liquid chromatography-quadrupole-orbitrap high resolution mass spectrometry. *Food Chem.* 361, 130147 <https://doi.org/10.1016/j.foodchem.2021.130147>.
- Yu, Q., Fan, L., 2021. Understanding the combined effect and inhibition mechanism of 4-hydroxycinnamic acid and ferulic acid as tyrosinase inhibitors. *Food Chem.* 352, 129369 <https://doi.org/10.1016/j.foodchem.2021.129369>.
- Zhao, J., Huang, L., Sun, C., Zhao, D., Tang, H., 2020. Studies on the structure-activity relationship and interaction mechanism of flavonoids and xanthine oxidase through enzyme kinetics, spectroscopy methods and molecular simulations. *Food Chem.* 323, 126807 <https://doi.org/10.1016/j.foodchem.2020.126807>.
- Zhao, L., Liu, J., Guo, R., Sun, Q., Yang, H., Li, H., 2017. Investigating the interaction mechanism of fluorescent whitening agents to human serum albumin using saturation transfer difference-NMR, multi-spectroscopy, and docking studies. *RSC Adv.* 7 (44), 27796–27806. <https://doi.org/10.1039/c7ra04008c>.
- Zeng, H.-j., Sun, D.-q., Chu, S.-h., Zhang, J.-j., Hu, G.-z., Yang, R., 2020. Inhibitory effects of four anthraquinones on tyrosinase activity: insight from spectroscopic analysis and molecular docking. *Int. J. Biol. Macromol.* 160, 153–163. <https://doi.org/10.1016/j.ijbiomac.2020.05.193>.
- Zhu, Y.-Z., Chen, K., Chen, Y.-L., Zhang, C., Xie, Y.-Y., Hider, R.C., Zhou, T., 2022. Design and synthesis of novel stilbene-hydroxypyridinone hybrids as tyrosinase inhibitors and their application in the anti-browning of freshly-cut apples. *Food Chem.* 385, 132730 <https://doi.org/10.1016/j.foodchem.2022.132730>.
- Zolghadri, S., Bahrani, A., Khan, M.T.H., Munoz-Munoz, J., Garcia-Molina, F., Garcia-Canovas, F., Saboury, A.A., 2019. A comprehensive review on tyrosinase inhibitors. *J. Enzym. Inhib. Med. Chem.* 34 (1), 279–309. <https://doi.org/10.1080/14756366.2018.1545767>.